Time Scales and pH Dependences of the Redox Processes Determining the Photocatalytic Efficiency of TiO_2 Nanoparticles from Periodic Illumination Experiments in the Stochastic Regime

C. J. G. Cornu, A. J. Colussi,* and M. R. Hoffmann*

W. M. Keck Laboratories, California Institute of Technology, Pasadena, California 91125

Received: November 26, 2002; In Final Form: January 10, 2003

The quantum yield, ϕ, of methyl orange photocatalytic oxidation on TiO_2 nanoparticles under periodic illumination drops from $\phi_{\tau_L \to 0}$ to $\phi_{\tau_L \to \infty}$ in two well-resolved steps at increasingly longer bright intervals, τ_L, when they are separated by sufficiently long dark periods, τ_D. The $\{\tau_{L1} < \tau_{L2}\}$ values at which the inflections occur depend exponentially, but with opposite trends, on the solution pH. The condition $\tau_D \gg \tau_L$ ensures charge sparsity, leads to a stochastic kinetics regime in which carrier recombination is minimized, and lets carriers manifest their dissimilar redox reactivities. The more reactive intermediates in acid (basic) media are ascribed to the photogenerated holes (electrons), the crossover occurring ca. pH 8. We found that $\phi_{\tau_L \to 0}$ and $\phi_{\tau_L \to \infty}$ coincide with the ϕ values measured under steady illumination at (γI_a) and I_a photon absorption rates, respectively, $\gamma = \tau_L/(\tau_L + \tau_D)$ being the duty cycle. The similar ϕ vs τ_L behaviors observed for methyl orange and formate are traceable to the dynamics of interfacial species. The photochemically relevant intermediates persist longer than a few milliseconds under typical conditions, i.e., several orders of magnitude longer that the plethora of transient spectroscopy signals (half-lives down to <1 ps) previously associated with these species.

Introduction

The charges separated upon band gap photoexcitation of semiconductors decay over many time scales.[1−8] Primary, possibly excited, carriers, hop through the material undergoing deactivation, trapping, and ultimately, recombination or redox transfer to interfacial species. Ultrafast kinetic spectroscopies have revealed transient optical signals, presumably associated with these processes, down to the subpicosecond scale.[8] The instantaneous generation of multiple carrier pairs per particle in pulsed high-power laser irradiation of dilute semiconductor suspensions leads to a fast decay initial phase in which charges recombine via bimolecular encounter, followed by increasingly slower kinetics over wide temporal scales. These behaviors are not representative, however, of the usual conditions prevailing in photocatalytic systems under weak illumination.[9] For example, diffuse reflectance infrared spectroscopy of illuminated dry TiO_2 powders shows that electrons persist for a few minutes upon illumination in the presence of moist oxygen, but up to days under vacuum or dry oxygen.[10,11] Some of the macroscopic transformations induced by solar illumination of TiO_2 surfaces also last for days under atmospheric conditions.[6,12,13]

In this context, it is critical to know whether the slow or the fast responses are actually associated with the photocatalytic activity of these materials.[5] Only a fraction of the primary carriers could possibly react at the interface, the remainder being trapped into slowly decaying inert species. Alternatively, the intermediates giving rise to the fast transients could be merely precursors of the reactive species being transformed at later stages. Below, we present new experimental evidence definitely supporting the latter scenario.[14]

Photochemistry under periodic illumination provides information on the lifetimes of reactive intermediates.[15−18] The technique involves quantum yield, ϕ, measurements under a periodic train of identical light pulses lasting τ_L, separated by dark periods of duration τ_D. In the case of a photochemical chain reaction involving a uniformly distributed, macroscopic number of molecules with spatially random photon absorption, ϕ is generally determined by the competition between the reactive and loss events of a single, rate-determining intermediate. If the kinetic orders with which the intermediate participates in these events are different, the resulting quantum yields depend explicitly on its average concentration, which is directly related to generation rates, i.e., to light absorption rates I_a: $\phi \propto I_a^m$, $m \neq 0$. When τ_L is long compared to the lifetime $\tau_{1/2}$ of the ϕ-controlling intermediate, the overall reaction rate R_p measured under intermittent light: $R_{p,\text{long }\tau}$, becomes the time average between the rate under full, steady illumination, $R_s = \beta I_{a,max}^n$ (β independent of I_a, $n = m + 1$), and the zero rate during the dark periods, i.e., $R_{p,\text{long }\tau} = \gamma b I_{a,max}^n$. In contrast, when τ_L is much shorter than $\tau_{1/2}$, the system behaves as if it were absorbing light at an effective photon absorption rate given by: $\langle I_a \rangle = \gamma I_{a,max}$. In this case, the overall rate becomes $R_{p,\text{short }\tau} = \beta(\gamma I_{a,max})^n$. Therefore, the ratio $R_{p,\text{long }\tau}/R_s$ changes from γ under slow modulation, to $R_{p,\text{short }\tau}/R_s = \gamma^n$ at sufficiently high modulation frequencies. If $n \neq 1$, $\gamma \neq \gamma^n$, and the transition between the limiting values will take place when τ_L is commensurate with $\tau_{1/2}$.[19,20] By definition: $\phi_{\tau_L \to \infty} = R_{p,\text{long }\tau}/\gamma I_{a,max} = \beta I_{a,max}^m$, $\phi_{\tau_L \to 0} = R_{p,\text{short }\tau}/\gamma I_{a,max} = \beta(\gamma I_{a,max})^m$.

In semiconductor photocatalysis, ϕ's typically vary from a I_a^0 to a $I_a^{-0.5}$ dependence with increasing photon flux.[21−25] The transition generally occurs about 1 sun equivalent (7×10^{-5} mol m^{-2} s^{-1}).[26] For immobilized photocatalysts at even higher photon fluxes, reaction rates may become mass-controlled rather than photon-controlled, depending on geometry and hydrodynamic conditions, i.e., $\phi \propto I_a^{-1}$.[23,26] In summary, three illumination regimes low ($m = 0$), intermediate ($m \sim -0.5$),

10.1021/jp027568+ CCC: $25.00
Published on Web 03/18/2003

and high ($m = -1$) photon absorption rates, can be expected in photocatalytic systems. Periodic illumination may have kinetic consequences in the intermediate regime.[27]

We previously reported that quantum efficiencies ϕ for formate oxidation in aqueous TiO_2 suspensions measured under variable-frequency periodic illumination contain direct information on the lifetimes of the photochemically relevant intermediates.[28] This technique interrogates the photochemical, rather than the optical response of the system to a controlled perturbation under actual reaction conditions. In this work, we explore further the nature of the intermediates involved in photocatalysis by applying the technique of periodic illumination to the bleaching of methyl orange in aqueous TiO_2 suspensions at various pH's. Quantum efficiencies, ϕ, span the entire accessible range under light modulation in the hertz to kilohertz frequency domain, reaching the ϕ values determined under steady-state illumination at the same average light intensity.[29−31] The ϕ vs τ_L dependence in experiments performed at small duty cycle values reveals the peculiar kinetic behavior of a system operating in a regime that exposes the differential reactivity between holes and electrons. Rather than a single rate-determining step, and a single transition between high- and low-frequency ϕ values, we observe two transitions, whose characteristic times are exponential functions of the solution pH.

Experimental Section

Experiments were performed by irradiation of TiO_2 suspensions contained in a jacketed, cylindrical fused silica reactor (26 mL, 2.5 cm optical path) fitted with flat windows. The light source was an ozone-free, 1000 W xenon arc lamp (Oriel). Its output traversed an IR filter (10 cm of water), a 320 nm high-pass filter, and a 340−380 nm band-pass filter, before illuminating the entire the reactor, which was maintained at 12 °C by means of a circulating bath. Light pulses were generated by means of either a mechanical shutter (Uniblitz VS14, 14 mm aperture, driven by a Uniblitz T132 controller) or an optical chopper (Oriel model 75155 with 2 model 75162 chopper blades offset with respect to each other, driven by a model 75095 chopper controller), located at the focal point of 2 focusing lenses. The shutter was used for pulsing below 5 Hz, and the chopper in the faster regime. The entrance aperture of the chopper was adjusted to yield the same transmittance of the shutter.

Titanium dioxide (Degussa P25) was used as received. Suspensions were prepared by 20 min sonication of P25 in deionized water. About 25 mL of these suspensions (6.4 mg L^{-1}), plus 1 mL of methyl orange (MO, J. T. Baker) stock solution (52 μM), was dispensed into the reaction cell. The resulting solutions (6.0 mg TiO_2 L^{-1}, 2 μM MO, pH = 6.0) were sparged with O_2 at 20 mL min^{-1} for 15 min prior to, and at 4 mL min^{-1} during, irradiation, while being stirred with a magnetic bar. The pH was adjusted to different values (2.5, 8.0, and 11.4) by adding a few drops of HCl (J. T. Baker, 36.5−38%) or NaOH (EM Science, 50%) at the beginning of the runs. It remained constant within ±0.2 pH units during the experiments.

The bleaching of MO was measured by withdrawing aliquots (0.5 mL) with a 0.2 μm polysulfone syringe filter (Gelman) at appropriate intervals. After the filtered aliquots were allowed to reach room temperature, MO was quantified by UV-absorption spectrophotometry (Hewlett-Packard 8452A diode array spectrophotometer) at 464 nm above pH = $pK_{a,MO}$ = 3.46,[32] and at 508 nm below. Absorbance vs concentration calibration curves were determined for each experiment. Recorded absorbances were corrected by subtracting the average background signal in the 600−650 nm range. Because MO bleaching strictly followed first-order kinetics up to 25% conversions, degradation rates were calculated from the least-squares regression of ln [MO] vs time data.

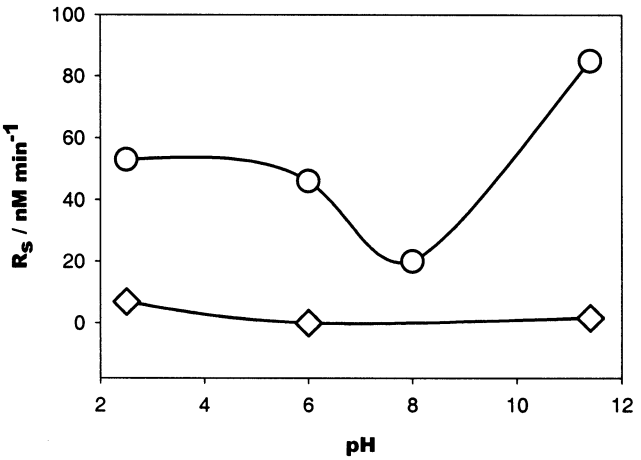

Figure 1. Methyl orange bleaching rates under steady illumination, R_s, in the presence and absence of TiO_2 vs pH: (◇) without TiO_2; (○) with 6 mg L^{-1} P25. Conditions: $[MO]_0 = 2$ μM, $T = 12$ °C, $I_a = 2.0$ μM^{-1} s^{-1}, O_2-saturated.

Light intensities were determined using (*E*)-α-[((2,5-dimethyl-3-furyl)ethylidene)isopropylidene]succinic anhydride (Aberchrome 540) as actinometer.[33] The maximum photon rate incident on the reactor at full illumination was $I_0 = 7.6$ μmol L^{-1} s^{-1}. The procedure used to estimate the fraction of the incident light absorbed by the photocatalyst particles has been described in detail elsewhere.[28] We found that 27% of the light is absorbed by the TiO_2 particles, i.e., $I_{a,max} = 2.0$ μmol L^{-1} s^{-1}. We verified that the photon rate incident on the cell in the dark, i.e., with the shutter closed, was about 3 orders of magnitude smaller than the incident photon rate with the shutter open. Hence, the effective photon absorption rate $\langle I_a \rangle$ under intermittent illumination is indeed given by $\langle I_a \rangle = \gamma I_{a,max}$. The incident photon rate under steady-state illumination was varied by interposing neutral density filters (Melles Griot).

Results

Light absorption by MO at pH > $pK_{a,MO} = 3.46$ centers at 464 nm, whereas absorption by the protonated form peaks at 508 nm.[32] In principle, MO may undergo photooxidation and/or photoreduction on illuminated TiO_2.[34−36] Because the product of MO reduction is a hydrazine derivative that absorbs at 247 nm,[35,36] the absence of new peaks in our experiments indicates that MO degradation largely proceeds by oxidative bleaching.

In a series of experiments we monitored the bleaching of MO under steady illumination at I_0 in the presence and absence of TiO_2, over the pH range covered in this work (Figure 1). There is no appreciable bleaching in the absence of TiO_2 at pH 6.0 or 11.4 (diamonds in Figure 1). However, the MO photodegradation rate (6.9 nM/min) at pH = 2.5 is about 13% of bleaching rates (53 nM/min) in the presence of TiO_2. Considering that our main goal is to clarify the mechanism of photocatalysis, rather than to obtain accurate values of ϕ, we neglected direct photolysis contributions to photocatalytic degradation and identify bleaching rates with photocatalytic oxidation rates in all cases. Steady-state rates in the presence of TiO_2, R_s, are shown in Table 1. Measured bleaching rates under full steady-state illumination lead to quantum yields of $10^4\phi = 4.4$, 3.8,

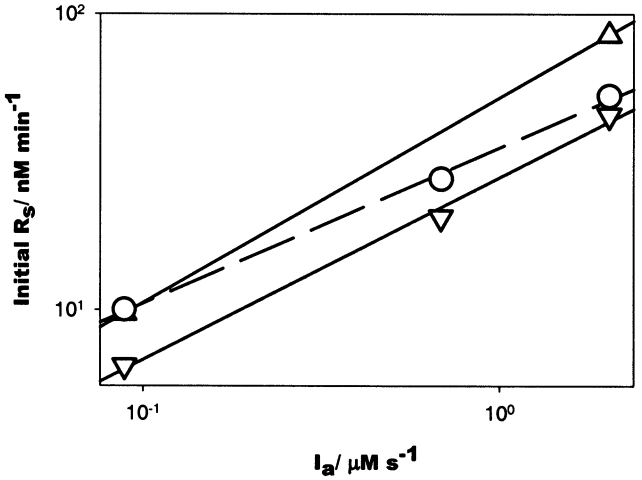

Figure 2. Methyl orange photocatalytic bleaching rates under steady illumination, R_s, vs I_a at various pH's: (○) pH 2.5; (▽) pH 6.0; (△) pH 11.4. Solid lines correspond to linear regressions to the data. Same conditions as in Figure 1.

TABLE 1: Methyl Orange Photocatalytic Bleaching Rates, $R_s \propto I_a^n$ under Steady-State Illumination as a Function of pH

pH	R_s [nM s^{-1}]	n
2.5	0.88	0.53
6.0	0.77	0.62
8.0	0.33	
11.4	1.42	0.69

1.7, and 7.0, at pH = 2.5, 6.0, 8.0, and 11.4, respectively, in good accord with previous literature reports.[34−36]

We examined the effect of the photon absorption rate, I_a, on bleaching rates under steady illumination, R_s, at different pH values, in the range $0.089 \leq I_a/\mu\text{mol L}^{-1}\text{ s}^{-1} \leq 2.0$. We found that bleaching rates are generally faster in acid or basic media than at about pH 8. Moreover, pH affects the n dependence of bleaching rates on I_a: $R_s = \beta I_{a,max}{}^n$ (Figure 2). The derived $0.5 \leq n \leq 1$ values (see Table 1) show that MO photocatalytic degradation rates under present conditions are neither photon-limited ($n = 1$) nor limited by mass transfer ($n = 0$) and, hence, that the technique of periodic illumination may provide kinetic information on the lifetimes of the intermediates determining the quantum efficiency of MO photocatalytic bleaching.

Methyl Orange Photocatalytic Bleaching under Periodic Illumination

A series of periodic illumination experiments was performed at $I_{a,max} = 2.0\ \mu\text{mol L}^{-1}\text{ s}^{-1}$, pH 6, $\gamma = 0.05$ and 0.35, by varying τ_L over 4 orders of magnitude (Figure 3). In these experiments: $\langle I_a \rangle = \gamma I_{a,max} = 0.10$ and $0.71\ \mu\text{mol L}^{-1}\text{ s}^{-1}$, at $\gamma = 0.05$ and 0.35, respectively, which are within the range of I_a values investigated in Figure 2. It is apparent that the ϕ's at $\gamma = 0.35$ and 0.05 are constrained by the values measured under steady-state illumination at $\langle I_a \rangle = 0.71$ and $0.10\ \mu\text{mol L}^{-1}\text{ s}^{-1}$, and that the transition between the two limiting values occurs in one and two steps, respectively.

In the $\gamma = 0.05$ case, two relatively sharp transitions are observed in the ϕ vs τ_L dependence: one at $\tau_L \sim 230$ ms (τ_{L2}), and a second one at $\tau_L \sim 22$ ms (τ_{L1}), which correspond to $\tau_D = 4.37$ s and 418 ms, respectively. These two transitions appear to merge into a broader, single one for $\gamma = 0.35$, which is centered at $\tau_L \sim 30$ ms ($\tau_D = 55.7$ ms). This behavior qualitatively resembles that reported for the photocatalytic oxidation of formate at pH 4.2 in the same setup (see Figure 5), which is about 100 times faster than MO bleaching under similar conditions.[28] Therefore, it represents a general feature of photocatalysis in TiO_2 suspensions. We attribute the lower ϕ values for MO to the fact that the numerous species representing the successive steps toward ($CO_2 + H_2O$) compete with the starting material for the same oxidative intermediates, a feature that is absent in formate oxidation.

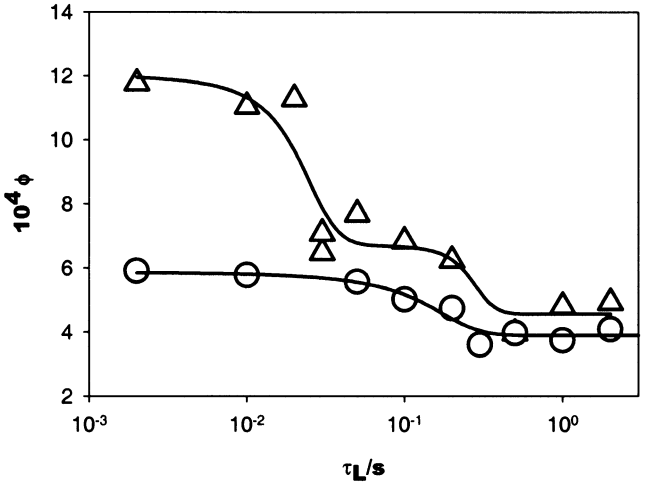

Figure 3. Quantum yields of methyl orange photocatalytic oxidation ϕ vs τ_L, the light period, under periodic illumination: (△) $\gamma = 0.05$, $\langle I_a \rangle = 0.10\ \mu\text{M}^{-1}\text{ s}^{-1}$; (○) $\gamma = 0.35$, $\langle I_a \rangle = 0.71\ \mu\text{M}^{-1}\text{ s}^{-1}$. The solid lines correspond to nonlinear least squares regressions based on double sigmoids. Same conditions as in Figure 1.

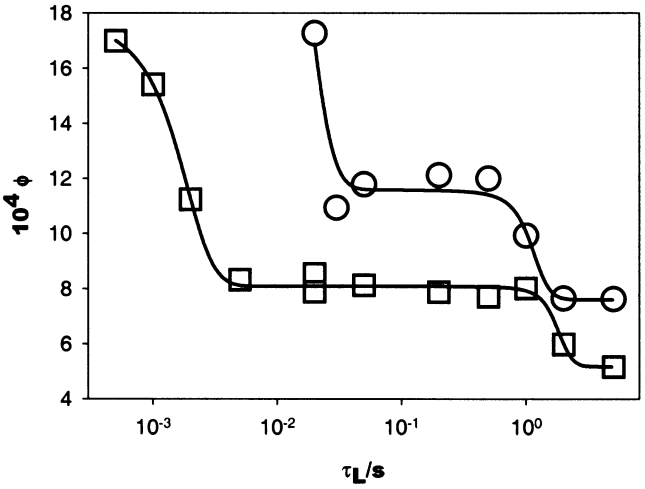

Figure 4. Quantum yields of methyl orange photocatalytic oxidation ϕ vs τ_L, the light period, under periodic illumination at $\gamma = 0.05$; (□) at pH 2.5; (○) at pH 11.4. The solid lines correspond to nonlinear least squares regressions based on double sigmoids. Same conditions as in Figure 1.

Influence of pH

We investigated the shift of τ_{L1} and τ_{L2} with pH, by performing a series of periodic illumination experiments at $\gamma = 0.05$. The results of experiments at pH 2.5 and 11.4 are shown in Figure 4. Two transitions are still observed in both cases, but the differences ($\tau_{L1} - \tau_{L2}$) are significantly different from those at pH 6.0. At pH 11.4, the two transitions ($\tau_{L1} = 15.6$ ms, $\tau_{L2} = 1.09$ s) fall within the 10 ms to 1 s τ_L window, whereas at pH 2.5 ($\tau_{L1} = 1.5$ ms, $\tau_{L2} = 1.75$ s) τ_{L1} is shortened 10-fold.

The strong correlation between experimental transition times τ_{L1} and τ_{L2} vs pH is shown in Figure 5, where τ_L's are the

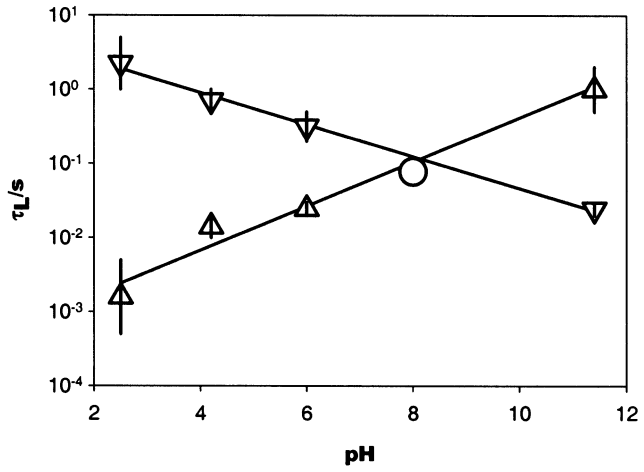

Figure 5. Transition lifetimes τ_L vs pH for photocatalytic oxidations. The "error" bars represent the width of the transitions. The solid lines are linear regressions: (△) τ_L's for oxidizing species; (▽) τ_L's for the reducing species. Experimental conditions as in Figure 1. The data at pH 4.2 are for the oxidation of 100 μM formate. The circle corresponds to MO oxidation at pH 8.0.

geometric mean values across each transition, and the vertical bars across the symbols are the transition widths. The regressions shown in Figure 5 correspond to log τ_L (▽) = 0.818−0.215 pH and log τ_L (△) = −3.359 + 0.298 pH and predict a crossover between τ_{L1} and τ_{L2} at pH 8.14. The predicted crossover was confirmed by a (limited) set of experiments at pH 8.0 (the circle in Figure 5). The data previously obtained for the degradation of formate at pH 4.2,[28] which have been included in Figure 5, confirm that the trend found for MO is general and, hence, that τ_{L1} and τ_{L2} may reflect the dynamics of common species residing on the surface of the photocatalyst.

Discussion

The exponential pH dependence of (τ_{L1}, τ_{L2}) allows us to draw some specific conclusions about the nature of the kinetically relevant intermediates. pH may affect photocatalytic rates by shifting the electrochemical potential of the TiO_2 surface.[37−40] The potential of a semiconductor in contact with aqueous media, i.e., the positions of the band edges, is shifted by −59 mV per pH unit at 298 K over a wide pH range. This Nernstian behavior has been observed for TiO_2 electrodes and colloidal particles. Thus, the redox potential of conduction band electrons e^-_{cb} becomes more negative at higher pH, a fact that increases the driving force for O_2 reduction

$$O_2 + e^-_{cb} \rightarrow O_2^- \qquad (1)$$

and the rate of reaction 1 at the TiO_2/solution interfaces, and as a consequence, shortens e_{cb} lifetimes. Conversely, a pH decrease will have a similar effect on the oxidizing power of valence band holes, their rates of interfacial electron capture from solution donors, and their lifetimes. In principle, however, interfacial redox processes may proceed by charge transfer events involving mobile electrons and holes, and also to and from trapped carriers whose potentials will also shift with pH. The actual chemical identity of the photochemically relevant intermediates may only be deduced from independent experiments (see below).

Under illumination, TiO_2 particles may also become charged with the less reactive carrier under the specific reaction conditions. This condition will be naturally realized under photon fluxes such that successive photons impinge on the particle before interfacial redox transfer removes the less reactive carriers. The excess charge will affect the electrochemical particle potential of the particle, the net effect being to increase the chemical potential of the excess carrier. Thus, for example, if the sluggish carrier were the electron, higher pH and larger photon fluxes will both enhance its reactivity. The dependence of electron-transfer rates on the overpotential, $E - E^{\Theta'}$, is given by the Butler−Volmer equation:[37−40]

$$k_{red} = k_0 \exp[-\alpha_{red} zF(E - E^{\Theta'})/RT] \qquad (2)$$

$$k_{ox} = k_0 \exp[\alpha_{ox} zF(E - E^{\Theta'})/RT] \qquad (3)$$

in which the rate constants for reduction and oxidation reactions, k_{red} and k_{ox}, depend exponentially on the surface potential, E; k_0 is the standard rate constant, and α_{red} and α_{ox} are the electron-transfer coefficients. Assuming that Butler−Volmer dependences also hold for suspended particles (the potential in this case is not varied by applying a potential bias, but by varying the pH of the surrounding solution or by charge buildup due to different reduction and oxidation rates), and considering that the lifetimes are inversely proportional to k_{red} and k_{ox}, eqs 2 and 3 predict an exponential dependence of the intermediates lifetimes on pH.

Thus, we propose that the transition times, τ_L, that decrease (increase) exponentially with increasing pH in Figure 5 belong to reducing (oxidizing) species. The reducing species has the longer lifetime below pH 8.2, whereas the converse is true for the oxidizing carriers. Because most experiments are carried out at pH 7 or lower, O_2 reduction is usually the slowest step,[37,41,42] a condition that is only incidental to the conditions employed, rather than being intrinsic of TiO_2.

The dual transitions observed at $\gamma = 0.05$ (Figures 3 and 4), and the fact that their positions are pH-dependent, imply that they are associated with reducing and oxidizing intermediates having different reactivities. At τ_L and τ_D longer than both lifetimes, the system is able to reach steady state during the light and in the dark periods. At τ_L and τ_D shorter than both lifetimes, the system behaves as if effectively subjected to steady-state illumination at γI_a. For τ_L and τ_D values between those extremes, one of the lifetimes is longer than τ_L and/or τ_D whereas the other one is shorter, resulting in intermediate bleaching rates. The larger the difference in the lifetimes of the oxidizing and reducing carriers, the longer the τ_L window in which an intermediate plateau is observed. Under present conditions, about 3 photons are absorbed by each particle per ms. The presence of more than one electron−hole pair per particle under illumination is revealed by the fact that $n \sim 0.6$, i.e, that carrier recombination competes with interfacial charge transfer. The first-order recombination of a single pair would have led to $n = 1$.

The varying lifetimes as a function of pH also shed light onto the mechanism of reaction. In contrast with the degradation of trichloroacetate and chloroethylammonium,[22] MO is photocatalytically degraded at faster rates at both high and low pH. Because the TiO_2 surfaces are positively charged below and negatively charged above pH ∼ 6.2, whereas MO is a zwitterion below and an anion above pH ∼ 4, the observed kinetic behavior apparently rules out MO adsorption on the TiO_2 surface as the determining factor. It would be unlikely that, under these circumstances, MO adsorption were pH-independent. The higher degradation rates and quantum yields observed at the extreme pH's can be explained, however, by the shift of the particle potential with pH, and the associated lifetimes of the reducing and oxidizing intermediates.

The observed lifetimes are too long to be those of valence band electrons and conduction band holes. Nosaka et al. reported a half-life of 17 s for superoxide at pH 11 in aqueous TiO_2 suspensions.[12] Similar experiments by Ishibashi et al. on TiO_2 films revealed a lifetime of superoxide of about 70 s in water.[6,13] It was observed that $O_2^{\bullet-}$ accumulates gradually with illumination time, reaching saturation after about 20 min under illumination at 1 μW cm^{-2}. The decay profile was found to obey first-order rate kinetics. More reactive species were also observed, disappearing in a few seconds, and were believed to be $OH^{\bullet}$ or/and surface-trapped holes.

Szczepankiewicz et al. determined that a hole could be localized at the TiO_2 surface as a surface-bound hydroxyl radical.[10] The assignment of the oxidizing intermediate to species such as hydroxyl radicals, surface-trapped holes, or surface-bound hydroxyl radicals, would explain why the observed lifetime is insensitive to the compound being degraded, because only a small fraction of those are used for the degradation, and their lifetimes are determined by other reactions, such as recombination with superoxide. Stopper and Dohrmann suggested that the long-lived (>2 μs) intermediates in optoacoustic calorimetric experiments carried out in aerated TiO_2 suspensions at pH 1−2.6 in the absence of oxidizable species were physisorbed OH_{aq} and $HO_{2,aq}$.[5] Further speculation about the identity of the intermediates involved is unwarranted.

Conclusions

Photochemical experiments under periodic illumination in the stochastic regime reveals two rate-determining intermediates having different lifetimes with opposite pH dependences. We assign these intermediates to the reducing and oxidizing species determining photocatalytic quantum yields on TiO_2/solution interfaces. The reducing species becomes more reactive at higher pH, the converse being valid for the oxidizing carrier, as a result of the shift in electrical potential of TiO_2 particles. Because the reactivity crossover occurs at pH 8.2, O_2 reduction will be the slowest, but not the ϕ-controlling step. The lifetimes of the intermediates are consistent with those of surface-bound, rather than surface-trapped, species, possibly O_2^- and OH radicals.

References and Notes

(1) Zhang, J. Z. *J. Phys. Chem. B* **2000**, *104*, 7239−7253.
(2) Bahnemann, D. W.; Hilgendorff, M.; Memming, R. *J. Phys. Chem. B* **1997**, *101*, 4265.
(3) Furube, A.; Asahi, T.; Masuhara, H.; Yamashita, H.; Anpo, M. *J. Phys. Chem. B* **1999**, *103*, 3120.
(4) Serpone, N.; Lawless, D.; Khairutdinov, R.; Pelizzetti, E. *J. Phys. Chem.* **1995**, *99*, 16655.
(5) Stopper, K.; Dohrmann, J. K. *Z. Phys. Chem.* **2000**, *214*, 555−572.
(6) Ishibashi, K. I.; Nosaka, Y.; Hashimoto, K.; Fujishima, A. *J. Phys. Chem. B* **1998**, *102*, 2117−2120.
(7) Rothenberger, G.; Moser, J.; Gratzel, M.; Serpone, N.; Sharma, D. K. *J. Am. Chem. Soc.* **1985**, *107*, 8054.
(8) Colombo, D. P.; Bowman, R. M. *J. Phys. Chem.* **1995**, *99*, 11752.
(9) Grela, M. A.; Colussi, A. J. *J. Phys. Chem.* **1996**, *100*, 18214−18221.
(10) Szczepankiewicz, S. H.; Colussi, A. J.; Hoffmann, M. R. *J. Phys. Chem. B* **2000**, *104*, 9842−9850.
(11) Szczepankiewicz, S. H.; Moss, J. A.; Hoffmann, M. R. *J. Phys. Chem. B* **2002**, *106*, 2922−2927.
(12) Nosaka, Y.; Yamashita, Y.; Fukuyama, H. *J. Phys. Chem. B* **1997**, *101*, 5822−5827.
(13) Ishibashi, K. I.; Fujishima, A.; Watanabe, T.; Hashimoto, K. *J. Phys. Chem. B* **2000**, *104*, 4934−4938.
(14) Behar, D.; Rabani, J. *J. Phys. Chem. B* **2001**, *105*, 6324−6329.
(15) Burnett, G. M., Melville, H. W., Friess, S. L., Lewis, E. S., Weissberger, A., Eds. *Physical Methods of Chemistry*; Interscience: New York, 1963; Vol. VIII, Part II, Chapter 20.
(16) Noyes, W. A. J.; Leighton, P. A. *The Photochemistry of Gases*; Reinhold: New York, 1941; Chapter 4.
(17) Haden, W. L.; Rice, O. K. *J. Chem. Phys.* **1942**, *10*, 445.
(18) Burnett, G. M.; Melville, H. W. *Nature* **1945**, *156*, 661.
(19) Bartlett, B. D.; Swain, C. G. *J. Am. Chem. Soc.* **1945**, *67*, 2273.
(20) Bartlett, B. D.; Swain, C. G. *J. Am. Chem. Soc.* **1946**, *68*, 2381.
(21) Okamoto, K.; Yamamoto, Y.; Tanaka, H.; Itaya, A. *Bull. Chem. Soc. Jpn.* **1985**, *58*, 2023.
(22) Kormann, C.; Bahnemann, D. W.; Hoffmann, M. R. *Environ. Sci. Technol.* **1991**, *25*, 494.
(23) Ohko, Y.; Ikeda, K.; Rao, T. N.; Hashimoto, K.; Fujishima, A. *Z. Phys. Chem.* **1999**, *213*, 33.
(24) Mills, A.; Wang, J. *Z. Phys. Chem.* **1999**, *213*, 49.
(25) Bahnemann, D.; Bockelmann, D.; Goslich, R. *Solar Energy Mater.* **1991**, *24*, 564.
(26) Ollis, D. F.; Pelizzetti, E.; Serpone, N. *Environ. Sci. Technol.* **1991**, *25*, 1523.
(27) Upadhya, S.; Ollis, D. F. *J. Phys. Chem. B* **1997**, *101*, 2625−2631.
(28) Cornu, C. J. G.; Colussi, A. J.; Hoffmann, M. R. *J. Phys. Chem. B* **2001**, *105*, 1351−1354.
(29) Sczechowski, J. G.; Koval, C. A.; Noble, R. D. *J. Photochem. Photobiol. A: Chem.* **1993**, *74*, 273−278.
(30) Buechler, K. J.; Nam, C. H.; Zawitowski, T. M.; Noble, R. D.; Koval, C. A. *Ind. Eng. Chem. Res.* **1999**, *38*, 1258−1263.
(31) Buechler, K. J.; Noble, R. D.; Koval, C. A.; Jacoby, W. A. *Ind. Eng. Chem. Res.* **1999**, *38*, 892−896.
(32) Skoog, D. A.; West, D. M.; Holler, F. J. *Fundamentals of Analytical Chemistry*, 7th ed.; Saunders College Publishing: Ft. Worth, TX, 1946.
(33) Heller, H. G.; Langan, J. R. *J. Chem. Soc., Perkin Trans. 2* **1981**, *2*, 341.
(34) Chen, L. C.; Chou, T. C. *J. Mol. Catal.* **1993**, *85*, 201.
(35) Brown, G. T.; Darwent, J. R. *J. Phys. Chem.* **1984**, *88*, 4955−4959.
(36) Brown, G. T.; Darwent, J. R. *J. Chem. Soc., Faraday Trans. 1* **1984**, *80*, 1631.
(37) Gerischer, H., Ollis, D. F., Al-Ekabi, H., Eds. *Photocatalytic Purification and Treatment of Water and Air*; Elsevier: Amsterdam, 1993; p 1.
(38) Gratzel, M. *Heterogeneous Photochemical Electron Transfer*; CRC Press: Boca Raton, FL, 1989; Vol. chapter 3.
(39) Bard, A. J.; Faulkner, L. R. *Electrochemical Methods. Fundamentals and Applications*; Wiley-Interscience: New York, 1980.
(40) Brett, C. M. A.; Oliveira-Brett, A. M. *Electrochemistry: Principles, Methods and Applications*; Oxford University Press: London, 1993.
(41) Kesselman, J. M.; Shreve, G. A.; Hoffmann, M. R.; Lewis, N. S. *J. Phys. Chem.* **1994**, *98*, 13385−13395.
(42) Gerischer, H.; Heller, A. *J. Phys. Chem.* **1991**, *95*, 5261−5267.